THE JOURNAL OF PHYSICAL CHEMISTRY B

Article

pubs.acs.org/JPCB

Dynamics of Geminate Rebinding of CO to Cytochrome c in Guanidine HCl Probed by Femtosecond Vibrational Spectroscopy

Jooyoung Kim, Jaeheung Park, Taegon Lee, Youngshang Pak, and Manho Lim*

Department of Chemistry and Chemistry Institute for Functional Materials, Pusan National University, Busan, 609-735 Korea

ABSTRACT: Femtosecond vibrational spectroscopy was used to probe the rebinding dynamics of CO to cytochrome c (Cytc) in 1.8 and 7 M guanidine HCl (GdnHCl) after photodeligation of the corresponding CO-bound protein in D_2O buffer (pD = 7.4) at 283 K. Geminate rebinding (GR) dynamics of CO to the folded Cytc in 1.8 M GdnHCl (*n*Cytc) is similar to that to chemically modified cytochrome c (cCytc), suggesting that the overall conformations of *n*CytcCO and *c*CytcCO are similar. About 86% of the dissociated CO molecules were geminately rebound to *n*Cytc nonexponentially within 1 ns. The efficient GR of CO to the folded Cytc can be attributed to the organized protein matrix near the active site of *n*Cytc that provides an efficient trap for the diffusing CO ligand after photodissociation. Although the concentration of *n*Cytc did not affect its GR yield of CO, GR yield of CO to the unfolded Cytc in 7 M GdnHCl (*u*Cytc) increased from 5 to 30% as the protein concentration increased from 0.3 to 9 mM. Time-resolved spectra of the ^{13}CO dissociated from both 9 mM *n*Cytc^{13}CO and 9 mM *u*Cytc^{13}CO showed a growing band with a peak at 2090 cm^{-1} on the picosecond time scale, which was assigned to ^{13}CO in D_2O solvent. At 1 ns, the fraction of the CO band in the solvent was about 10% of the nascent photodeligated protein in *n*Cytc and more than 50% in the concentrated *u*Cytc. Whereas a small opening in the active site of *n*Cytc is responsible for the ultrafast escape of CO to solution in the folded protein, a large fraction of the CO escape to the solvent in *u*Cytc results from the denatured structure of the active site in the unfolded protein. The spectrum of the CO dissociated from the concentrated *u*CytcCO contained a band that decayed as efficiently as that for the folded protein, suggesting that some fraction of *u*CytcCO might form aggregates even in 7 M denaturant, such that the aggregate acts as an efficient trap for the diffusing CO after deligation. No hint of precipitate in the concentrated *u*CytcCO and protein refolding upon dilution of the GdnHCl indicate that the aggregate does not grow continuously but remains as a soluble oligomer. The delayed appearance of the solvated CO and the inefficient GR of CO in *u*CytcCO suggest that the monomeric unfolded CytcCO so loosely arranged that the protein matrix cannot trap CO efficiently but the bound CO is still buried within hydrophobic residues even under the harsh denaturation condition.

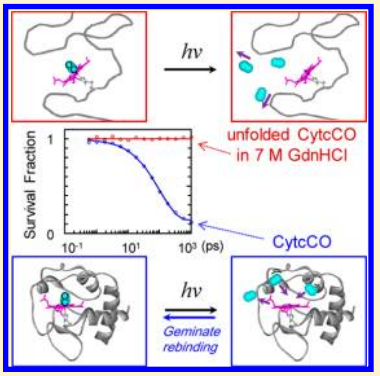

INTRODUCTION

Unfolded states of proteins play important roles in various critical biological phenomena, ranging from the onset of neurodegenerative diseases to the regulation of cellular activity.[1,2] Characterizing the structure and dynamics of unfolded proteins is important for understanding not only these biological phenomena but also protein folding itself.[2] Since a detailed investigation of unfolded proteins is often hampered by their propensity to aggregate and/or the lack of structural and dynamic probes,[3] the structure and dynamics of unfolded proteins are much less understood compared to those of folded proteins.[4,5]

The rebinding of CO after the photolysis of CO-bound heme proteins such as myoglobin (Mb) and hemoglobin (Hb) has served as a model system for examining how a protein's structure and dynamics are related to its function.[6−9] The rebinding of CO to cytochrome c (Cytc), a ubiquitous small soluble electron transfer protein carrying one heme cofactor, was also investigated in a comparative study exploring how Mb modulates the rate of CO binding to the heme.[10] In contrast to Mb and Hb, native Cytc cannot bind CO, because its heme is coordinated by two axial ligands, His-18 and Met-80.[11] A chemically modified Cytc (*c*Cytc) in which the sulfur atom of Met-80 has been carboxymethylated after disruption of the Met-Fe bond can bind an external neutral CO ligand[12] and was used to study CO rebinding.[10,11,13,14] The rebinding of CO to *c*Cytc was more than 1000 times faster than that to native Mb and even faster than that to a model heme, microperoxidase-8 (Mp), in viscous solutions.[10] The *c*Cytc does not have a structure similar to the primary docking site (PDS) in Mb, a hydrophobic cavity in the proximity of the heme group that suppresses the binding of CO by constraining the motion of CO orientationally and spatially.[9] The organized protein matrix of the folded *c*Cytc was suggested to serve as an efficient trap for the diffusing CO and thus accelerate geminate rebinding (GR).[10] As shown in the unfolding curve of Cytc (figure 1), Cytc can also bind CO when, first, it is unfolded by guanidine HCl (GdnHCl), and then, the denaturant is diluted to a folding concentration.[15,16] The addition of the carboxymethyl group in *c*Cytc can disturb the distal area of the active site, which can destroy the PDS-like structure that might exist in the native Cytc. Thus, a rebinding study using CO-ligated Cytc without chemical modification is useful for evaluating the

Received: February 10, 2013
Revised: March 24, 2013
Published: March 27, 2013

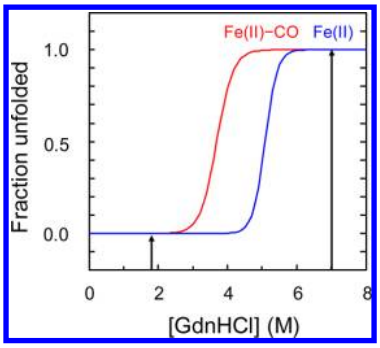

Figure 1. Unfolding curves of ferrous cytochrome c (blue line) and CO-bound ferrous cytochrome c (red line). The arrows indicate GdnHCl concentrations of 1.8 and 7 M, where *n*CytcCO and *u*CytcCO, respectively, were prepared. Unfolding curves are from ref 16.

influence, if any, of the added carboxymethyl group in *c*Cytc on the GR of CO to the protein.

Recently, we probed the rebinding dynamics of photodeligated CO to Mb unfolded by 4 M GdnHCl (*u*Mb).[5] The rebinding of CO to the *u*Mb was more than 1000 times faster and more efficient than that to the native Mb. Furthermore, no spectrum for CO in bulk solution was observed in 1 ns, indicating that the dissociated CO resides within hydrophobic sites of the *u*Mb.[5] The efficient GR of CO in the *u*Mb was attributed to trapping of the CO by the unfolded protein matrix and the destruction of the PDS present in the native Mb. The absence of solvated CO and the efficient GR of the dissociated CO suggested that the unfolded polypeptide chain wraps around the distal side of the heme where the bound CO protrudes and the wrapping facilitates GR of the CO by delaying the diffusion of the dissociated CO. It was concluded that the unfolded MbCO does not have a fully extended structure exposing the bound CO, even under complete denaturation conditions, for example, in the presence of 4 M GdnHCl.[5] This conclusion contrasts with the notion that the unfolded protein in harsh denaturant has a fully extended structure, as depicted in the literature.[15] Whereas the unfolded protein in a harsh denaturant is known to be a structureless random chain,[17−20] it has also been suggested that unfolded CytcCO is not necessarily a random coil.[3,21] Structural information about the unfolded protein can be useful in reconciling this discrepancy.

According to the GdnHCl folding curve, both Cytc and CytcCO are completely unfolded in 6 M or higher GdnHCl concentrations. Since the vibrational spectrum of a gaseous ligand has been demonstrated to be very sensitive to its environment,[9,10,22−26] the spectrum of the dissociated CO can be used as a local probe of the internal structure of an unfolded protein as well as an excellent probe for the details of the ligand's rebinding dynamics.[5] The rebinding dynamics of photodeligated CO from fully unfolded Cytc can reveal the structure of the unfolded protein as well as the dynamics of the associated ligand.

Here femtosecond vibrational spectroscopy was used to probe the rebinding dynamics of CO after the photodeligation of CO from CytcCO in 1.8 M (*n*CytcCO) and 7 M (*u*CytcCO) GdnHCl at 283 K. We found that most of the CO dissociated from *n*CytcCO was geminately rebound in 1 ns. The GR of CO to *n*Cytc is similar to that to *c*Cytc; a small fraction of the dissociated CO escapes to the solvent on a time scale of picoseconds, and most of the remainder, trapped by the organized protein matrix, geminately rebound within 1 ns. The overall structure of *n*CytcCO is likely the same as that of *c*CytcCO. The GR of CO to *u*Cytc became more efficient as the concentration of the protein increased from 0.3 to 9 mM; the GR yield increased from 5 to 30%. When the vibrational band of CO in *u*CytcCO was decomposed into three Gaussian bands, one band showed complete GR in 1 ns and the other two did not exhibit any GR. These observations suggest that most of CytcCO in 7 M GdnHCl, a complete unfolding condition, has a structure that cannot trap the dissociated CO to rebind but, as the concentration of the protein increases, a subset of *u*CytcCO forms such a structure, so that the dissociated CO is as efficiently trapped as in the folded protein. The subset likely arises from a soluble aggregate of *u*CytcCO.

MATERIALS AND METHODS

The time-resolved vibrational spectrometer used here has been described elsewhere in detail.[27] Briefly, a visible pump pulse and a mid-IR probe pulse were generated using two optical parametric amplifiers (OPA) that were pumped by a commercial Ti:sapphire amplifier. A 3 μJ pump pulse at 575 nm was produced by frequency doubling of a signal pulse of one OPA, and a tunable mid-IR probe pulse was produced by difference-frequency mixing of the signal and idler pulses of the other OPA. The isotropic absorption spectrum was obtained by setting the polarization of the pump pulse at the magic angle (54.7°) relative to the probe pulse. The broadband transmitted probe pulse was detected by a 64-element $N_2(l)$-cooled HgCdTe array detector. The array detector was mounted in the focal plane of a 320 mm monochromator with a 150 *l*/mm grating, resulting in a spectral resolution of ca. 1.6 cm^{-1}/pixel at 2070 cm^{-1}. The instrument response function was typically 150 fs.

A solution of 0.3−9 mM Cytc^{13}CO in 7 M GdnHCl was prepared by dissolving lyophilized horse heart ferric cytochrome c (Sigma) in concentrated GdnHCl (Aldrich) in D_2O buffered with 0.1 M phosphate (pD = 7.4). The solution was thoroughly deoxygenated by purging with ^{13}CO (Aldrich, 99.3% ^{13}C), equilibrated with 1 atm of ^{13}CO, and reduced with 3-fold equivalents of freshly prepared sodium dithionate (Aldrich). To ensure complete CO ligation, the reduced solution was stirred under 1 atm ^{13}CO for about 10 min. A solution of 1−9 mM Cytc^{13}CO in 1.8 M GdnHCl was prepared at a high concentration of GdnHCl to facilitate ligation by unfolding the protein, and then the solution was diluted to recover the folded protein. As can be seen in Figure 1, CytcCO maintains a folded structure in solutions with less than 2.5 M GdnHCl concentration. A 4-fold dilution of our sample, CytcCO in 0.45 M GdnHCl, showed the same spectral characteristics as CytcCO in 1.8 M GdnHCl (data not shown), confirming that the protein was in the folded structure.[21] UV−vis and FT-IR spectroscopy confirmed the formation of *n*CytcCO and *u*CytcCO. The *n*CytcCO sample was loaded in a gastight flowing sample cell with an 80 μm path length Teflon spacer and two CaF_2 windows. The *u*CytcCO sample was loaded in a gastight 80 μm path length rotating sample cell to minimize sample usage (see Discussion). During data collection, the sample was flowed or the sample cell was rotated sufficiently fast that each photolyzing laser pulse illuminated a fresh volume of the sample. Throughout the experiments, UV−vis and FT-IR spectroscopy were employed to check the integrity and the concentration of the samples. The temperature of the sample cell was kept at 283 ± 1 K using a circulating coolant bath through the sample cell Al block. The sample was prepared in D_2O using ^{13}CO to isotopically shift the spectrum of interest into a region with greater IR transmission.

dx.doi.org/10.1021/jp401481q | J. Phys. Chem. B 2013, 117, 4934−4944

Since the vibrational band of photodeligated CO had a much lower extinction coefficient than bound CO,[10] about 9 mM of CytcCO was required for the time-resolved vibrational spectra of photodeligated CO under our experimental conditions. In a 9 mM solution, the protein occupies more than 10% of the sample volume; therefore, concentration-dependent behavior might be observed in the GR kinetics as well as structural change. Thus, FT-IR and time-resolved spectra of CO in CytcCO were collected at various protein concentrations and analyzed.

RESULTS

Figure 2 displays the FT-IR spectra of the CO stretching mode in Cytc^{13}CO in 1.8 and 7 M GdnHCl solutions at room

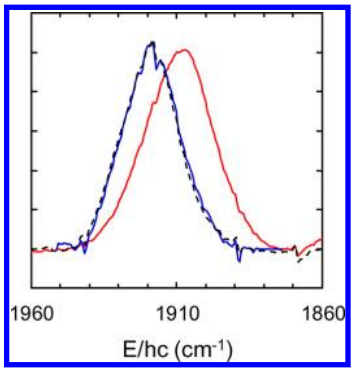

Figure 2. FT-IR spectra of CO stretching mode in Cytc^{13}CO in 1.8 M GdnHCl (black dashed line) and 7 M GdnHCl (red line) solutions at room temperature. The CO band in refolded CytcCO (blue line) overlaps that in *n*CytcCO. For better comparison, the refolded band was normalized to that in *n*CytcCO. Spikelike structures in the spectrum arise from water vapor absorption due to incomplete purge.

temperature. The CO band in *n*Cytc^{13}CO showed a single peak at 1919 cm^{-1} with a full width at half-maximum (fwhm) of 23 cm^{-1} and that in *u*Cytc^{13}CO also had a single peak at 1909 cm^{-1} with an fwhm of 28 cm^{-1}. A redshift in the CO band was also observed upon the thermal unfolding of Cytc.[28] As mentioned, to explore any concentration dependence of the sample, spectra were taken at various protein concentrations while maintaining the GdnHCl concentration. Whereas the CO band was virtually identical in 1 and 9 mM *n*Cytc^{13}CO, it was red shifted by about 3 cm^{-1} when the concentration of *u*Cytc^{13}CO increased from 0.3 to 9 mM. When 9 mM Cytc^{13}CO in 7 M GdnHCl solution was diluted to 1.8 M GdnHCl to evaluate reversibility, the CO band became identical to that in *n*Cytc^{13}CO (Figure 2), implying that the unfolded protein was refolding upon the dilution of GdnHCl. There was no detectable precipitate in 9 mM *u*CytcCO even after a few days of incubation. The concentration-dependent behavior of *u*CytcCO might arise from the formation of aggregates of unfolded CytcCO in 7 M GdnHCl. The refolding of the 9 mM *u*CytcCO upon dilution and the lack of precipitation suggest that, if it forms, the aggregate of CytcCO in 7 M GdnHCl does not grow continuously and then precipitate, but it remains a soluble oligomer in the concentration range explored (0.3−9 mM).

Figure 3 shows the time-resolved vibrational spectra of the ^{13}CO stretching mode of 1 mM Cytc^{13}CO in 1.8 M GdnHCl solution at 283 K after photoexcitation with a 575 nm pulse. The featureless background offset in the transient spectra was modeled with a linear equation and subtracted from the measured spectra. The featureless background is known to

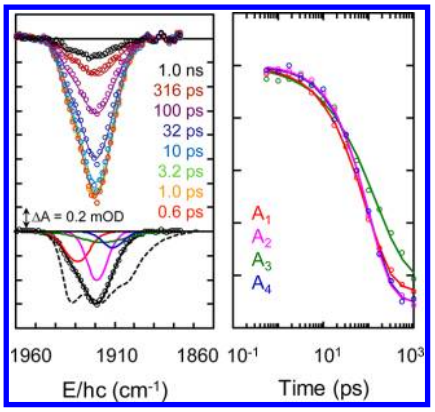

Figure 3. (Left panel) Representative time-resolved vibrational spectra of the ^{13}CO stretching mode of 1 mM Cytc^{13}CO in 1.8 M GdnHCl solution (*n*CytcCO) at 283 K after photolysis with a 575 nm pulse. The solid lines are a sum of four Gaussians, and the pump−probe delay is color-coded. For clarity, a linear background has been subtracted from the measured spectra (see text). Four Gaussian components in the transient CO spectra at 0.3 ps are also shown in the lower part. The transient spectrum of *c*CytcCO at 0.3 ps (black dashed line) is overlapped with that of *n*CytcCO to show the difference in the spectral width. (Right panel) Amplitude changes of four Gaussians after photolysis of 1 mM *n*CytcCO at 283 K. Each Gaussian component is color-coded with the corresponding kinetics component in the left panel and denoted as A_1, A_2, A_3, and A_4 in order of increasing wavenumber. The amplitude is normalized for better comparison. The GR kinetics was fit to the three-state model (solid lines).

arise mainly from the spectral change of the solvent resulting from the thermal relaxation of the protein.[9,25,29] The negative-going features (bleach), appearing faster than the time resolution of the instrument, arise from the loss of bound CO (denoted as the A state). Instantaneous bleach implies that the photodissociation of CO is ultrafast, as observed in other CO-bound heme proteins such as HbCO and MbCO.[30] The magnitude of the bleach is proportional to the population of the photodeligated Cytc, and the picosecond recovery of the bleach results from the rebinding of CO. Since the bimolecular rebinding of CO to heme proteins proceeds on the millisecond time scale,[31,32] the decay of the bleach amplitude could be attributed solely to GR within our experimental time span of 1 ns; thus, the bimolecular contribution will be neglected hereafter. The shape of the bleach changed slightly with time, suggesting that the spectrum consists of several bands, each having different GR kinetics. At least four Gaussians were required to follow the spectral evolution of the bleach in *n*CytcCO, and the decay kinetics of each Gaussian was slightly different (Figure 3). Distinct vibrational bands of the bound ligand in heme proteins are known to arise from conformational substates of the protein.[33,34] Therefore, *n*CytcCO in GdnHCl has at least four conformational substates. Band-dependent rebinding kinetics indicates that the CO rebinding to Cytc in GdnHCl solution depends on the conformation of the protein, and the interconversion among the conformational substates is slower than the GR. We also obtained time-resolved vibrational spectra of 9 mM *n*Cytc^{13}CO and found that the GR kinetics and the spectral characteristics for 9 mM *n*Cytc^{13}CO were virtually identical to those of 1 mM *n*Cytc^{13}CO.

Time-resolved vibrational spectra of the ^{13}CO stretching mode of 0.3−9 mM Cytc^{13}CO in 7 M GdnHCl solution at 283 K were also obtained after photoexcitation with a 575 nm pulse and analyzed similarly to the data for *n*CytcCO. Three Gaussians

dx.doi.org/10.1021/jp401481q | J. Phys. Chem. B 2013, 117, 4934−4944

(denoted as A_5, A_6, and A_7, in order of increasing wavenumber) were required to follow the spectral evolution of the bleach in *u*CytcCO. As the concentration of *u*CytcCO increased from 0.3 to 9 mM, the contribution of the A_5 band decreased from 85 to 66% and that of the A_6 band increased from 5 to 30%. Among the three Gaussian components, two Gaussian bands in the wings on both sides (the A_5 and A_7 bands) did not decay in 1 ns, and the remaining Gaussian band (the A_6 band) decayed nonexponentially (Figure 4). The A_6 band decayed completely in 1 ns and its

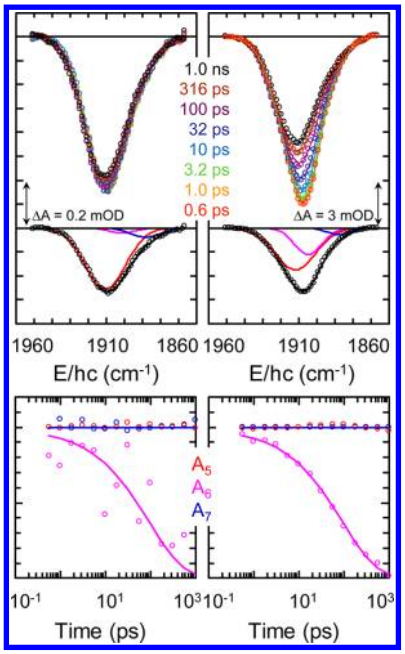

Figure 4. (Upper panels) Representative time-resolved vibrational spectra of the ^{13}CO stretching mode of Cytc^{13}CO in 7 M GdnHCl solution (*u*CtycCO) at 283 K after photolysis with a 575 nm pulse. The solid lines are the sum of three Gaussians and the pump−probe delay is color-coded. For clarity, a linear background has been subtracted from the measured spectra (see text). Three Gaussian components in the transient CO spectra at 0.3 ps are also shown in the lower part. (Lower panels) Amplitude changes of three Gaussians after photolysis of *u*CytcCO. Each Gaussian component is color-coded with the corresponding kinetics component in the upper panel and denoted as A_5, A_6, and A_7 in order of increasing wavenumber. The amplitude is normalized for better comparison. The GR kinetics of the A_6 band was fit to the three-state model (solid lines). The left and right panels correspond to 0.3 and 9 mM *u*CytcCO, respectively.

decay kinetics was found to be independent of the concentration of the protein. The contribution of the A_6 band to the spectrum at 0.3 ps was 5, 8, 12, 19, and 30% in 0.3, 0.5, 1, 3, and 9 mM *u*CytcCO, respectively. The gradual increase of the decaying component resulted in the increase of the overall GR yield of CO to *u*Cytc with the protein concentration. Evidently, most of the unfolded CytcCO in 7 M GdnHCl adopted conformations that did not show any GR of CO in 1 ns, but as the protein concentration increased, *u*CytcCO started to adopt a conformation that exhibited complete GR of CO in 1 ns. One possible conformation that could undergo GR is an aggregate of the unfolded CytcCO. Because there were no detectable precipitates, even in 9 mM *u*CytcCO after a few days of incubation, and the protein refolded upon dilution of the GdnHCl, the aggregate must have remained as a soluble oligomer without growing continuously.

As can be seen in Figures 4 and 5, the overall as well as band-position dependent rebinding kinetics of CO to Cytc are highly

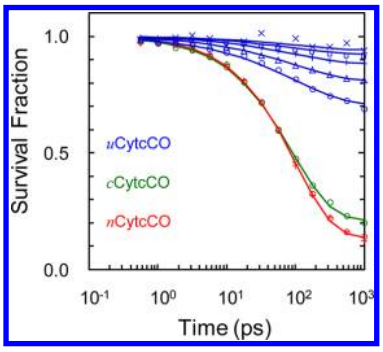

Figure 5. Change in survival fraction of deligated heme in *n*CytcCO (red), *u*CytcCO (blue), and *c*CytcCO (green)[10] in D_2O at 283 K after photolysis with a 575 nm pulse. The concentration of the protein was 0.3 (crosses), 0.5 (open squares), 1 (pluses), 3 (open triangles), and 9 mM (open circles). The three-state model was used to fit the GR kinetics (solid lines).

nonexponential. Ligand rebinding to heme proteins has been described by a three-state kinetic model[10,31,35]

$$\underset{\text{(A state)}}{\text{CytcCO}} \xleftarrow{k_{CA}} \underset{\text{(C state)}}{\text{Cytc:CO}} \underset{k_{SC}}{\overset{k_{CS}}{\rightleftarrows}} \underset{\text{(S state)}}{\text{Cytc + CO}}$$

where Cytc:CO represents the geminate pair state (denoted as the C state), and Cytc + CO represents the state in which the dissociated CO escapes into the solvent (denoted as the S state). Because bimolecular rebinding in 1 ns is neglected, the change in the normalized absorbance, the magnitude of which represents the fraction of deligated Cytc after photolysis, can be expressed as $\Delta A(t)/\Delta A(0) = I_g e^{-(t/t_g)^{\beta}} + (1 - I_g)$.[35] Here, I_g and τ_g represent the GR yield and time constant, respectively. The exponent, β, which satisfies $0 < \beta \leq 1$, accounts for the nonexponentiality that arises from fast relaxation of the protein that modifies the rebinding barrier and/or the distribution of the rebinding barrier because of the inhomogeneous protein conformation.[35] When the GR kinetics is exponential (i.e., $\beta = 1$), the fundamental time constants defined in the three-state model are related to the observed τ_g and I_g: $\tau_{CA} = 1/k_{CA} = \tau_g/I_g$ and $\tau_{CS} = 1/k_{CS} = \tau_g/(1 - I_g)$.[31,35] The stretched exponential can be viewed as a distribution of ordinary exponentials; then, the mean time of the distribution, $\langle\tau\rangle$, is readily calculated using $\langle\tau\rangle = \Gamma(\beta^{-1})\tau/\beta$, where $\Gamma(x)$ is the gamma function.[36] The overall GR kinetics of CO to *n*Cytc was fitted to 0.86 exp $(-(t/100\text{ ps})^{0.79})$ + 0.14, and the GR kinetics of CO to the A_6 in *u*Cytc was fitted to exp $(-(t/100\text{ ps})^{0.57})$. From the fitted parameters, the time constants were calculated: $\langle\tau_g\rangle$ = 120 ps, $\langle\tau_{CA}\rangle$ = 140 ps, and $\langle\tau_{CS}\rangle$ = 830 ps for *n*CytcCO; and $\langle\tau_g\rangle$ = 160 ps, $\langle\tau_{CA}\rangle$ = 160 ps for the A_6 in *u*CytcCO. As can be seen in Figure 5, the overall rebinding of CO to *n*Cytc is much more efficient than that to *u*Cytc, but similar to that to *c*Cytc.

Figure 6 shows the transient IR spectra of ^{13}CO photolyzed from 9 mM Cytc^{13}CO in 1.8 and 7 M GdnHCl. As mentioned, a protein sample concentration of at least 9 mM was necessary to obtain a reasonable signal for the photodeligated CO, which has a much lower extinction coefficient than bound CO in CytcCO. The ultrafast appearance of the positive feature indicates that these spectra arise from CO located near the Fe atom of the heme. These were denoted as the C states to differentiate them from the B-state spectra observed after photolysis of MbCO and HbCO, where CO resided in the well-structured PDS that plays a

dx.doi.org/10.1021/jp401481q | J. Phys. Chem. B 2013, 117, 4934−4944

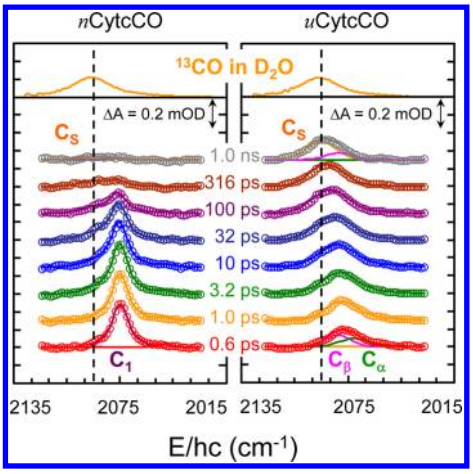

Figure 6. Representative time-resolved vibrational spectra of ^{13}CO photolyzed from 9 mM *n*Cytc^{13}CO (left panel) and *u*Cytc^{13}CO (right panel) at 283 K. The equilibrium spectrum of solvated ^{13}CO in D_2O is also shown for comparison, and its peak position is marked by the dashed vertical line. The data (○) were fitted to several bands, two bands (denoted as C_1 and C_S) in *n*Cytc^{13}CO and three bands (denoted as C_α, C_β, and C_S) in *u*Cytc^{13}CO, plus their hot bands (see text). The spectra at 0.3 ps and 1 ns are decomposed into their components. For clarity, a quadratic background was subtracted from the measured spectra, and the spectra were offset to avoid overlap.

significant role in suppressing the GR of CO in these ligand-binding proteins.[5,9,10] Transient spectra of CO photolyzed from CytcCO revealed a strong spectral evolution for both *u*CytcCO and *n*CytcCO. The evolving spectra were modeled with a main band near 2075 cm^{-1} plus its red-shifted replica that resulted from a vibrationally hot band with an anharmonic shift of 25 ± 1 cm^{-1} and a vibrational relaxation (VR) time of 600 ± 300 ps.[24,25,37] The fast decaying data with a low signal-to-noise (S/N) ratio could not be used to determine the VR time of the deligated CO within Cytc accurately, and thus, the VR time was set to 600 ps in the final fitting, which was the value for the deligated CO within Mb. When the VR time was set to either 300 or 900 ps in the fitting, the recovered parameters were negligibly affected. The transient spectra at 1 ns resembled the spectrum of ^{13}CO dissolved in D_2O (denoted as C_S),[38] suggesting that the majority of this spectral feature at 1 ns resulted from CO that escaped to the bulk solution. A quadratic polynomial was used to model the featureless background resulting from the change in the solvent spectrum due to thermal relaxation of the protein. It was subtracted from the measured spectra for clarity. The nascent vibrationally excited CO population was found to be 5 ± 1%, which was similar to the value obtained in *c*Cytc as well as in Mb.[10,22] The evolution and the shape of the transient spectra of the dissociated CO obtained after photolysis of *n*CytcCO are similar to those of *c*CytcCO but are quite different from those of *u*CytcCO. We modeled the transient spectra of *n*CytcCO in the same way as those of *c*CytcCO: an evolving C_1 band plus the C_S band.[10] The C_1 band arises from CO in the hydrophobic cavity of *n*Cytc located in immediate proximity to the Fe atom and the C_S band from CO dissolved in water that has escaped to bulk solution. The C_1 band was thought to arise from CO in several ill-structured cavities.[10] The position of the C_1 band shifted blueward from 2075 cm^{-1} at 1 ps to 2076.3 cm^{-1} at 1 ns with kinetics described by a log function, 0.5 log(t), which was consistent with the band shift observed in *c*Cytc with the function 0.6 log(t).[10] The band shift has been suggested to arise from the conformational relaxation of the protein following the deligation of CO from the folded CytcCO. Efficient nonexponential decay of the C_1 band and a nanosecond decay with ensuing picosecond growth of the C_S band in *n*Cytc (figure 7) were also similar to those observed in *c*Cytc.

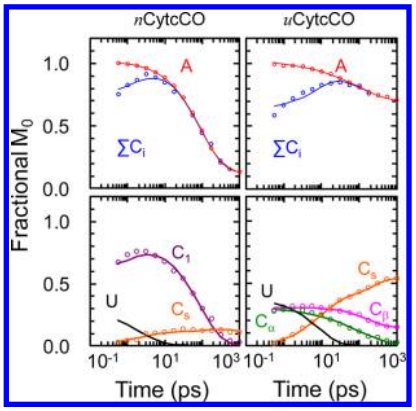

Figure 7. (Upper panels) Time-dependent change in the fractional zeroth moment (M_0, the integrated area) of the vibrational band of bound CO (A state, red) and deligated CO (B state, blue) in 9 mM *n*CytcCO and *u*CytcCO at 283 K. The total M_0 for the C states is scaled to match that of the A state without exceeding it. (Lower panels) Fractional M_0 change of deligated CO in each state of *n*CytcCO and *u*CytcCO. The U state represents the undetectable state for the deligated CO (see discussion). The data (○) were fitted to a multisite model with nonexponential kinetics using the stretched exponential function (see text).

The transient CO spectra of *u*Cytc exhibited an evolving broad main band. The broader band in *u*Cytc likely arose from the more heterogeneous conformation of the unfolded protein. Since the unfolded protein is unlikely to have a systematic conformational relaxation that causes a band shift after deligation, the evolution of the main band in *u*CytcCO was modeled using two bands with changing amplitudes at fixed positions (denoted as C_α and C_β) plus the C_S band. The C_α band was located at 2072 cm^{-1} with a 23 cm^{-1} fwhm, and the C_β band, at 2080 cm^{-1} with a 16 cm^{-1} fwhm. Both bands were broader than or equal to the band observed in *n*CytcCO, whose C_1 band was located at 2075−2076.3 cm^{-1} with a 16 cm^{-1} fwhm. As can be seen in figure 7, the time-dependent changes of the main bands and the C_S band in *u*Cytc were quite different from those in *n*Cytc. For *n*Cytc, the unbound CO at 1 ns constituted about 14% of the dissociated CO, and the majority of it was dissolved in solvent. For *u*Cytc, the unbound CO at 1 ns was about 70% of the dissociated CO, about three-fourths of which were in solvent; the remainder was in the C_β state. Interestingly, the decay kinetics of the C_α band in *u*Cytc mimicked that of the A_6 band in the bound CO, suggesting that the conformation causing the GR of CO in *u*Cytc gives rise to the C_α band. We tried to fit the main band of the photolyzed CO from *u*CytcCO with a shifting band plus the C_S band, as we did for *n*Cytc, and found that the main band shifted blueward by 3.3 cm^{-1} in 1 ns with an ever-increasing rate. The magnitude of the shift was too large compared with the magnitude of *n*Cytc and *c*Cytc, 1.3−1.8 cm^{-1} in 1 ns,[10,39] and the trend of the shift could not be accounted for by conformational relaxation.

dx.doi.org/10.1021/jp401481q | J. Phys. Chem. B 2013, 117, 4934−4944

DISCUSSION

Although the CO vibrational band in *n*CytcCO was much narrower than that in *c*CytcCO (figure 3), the same number of Gaussians was required to reproduce the spectral evolution of *n*CytcCO as was required for *c*CytcCO, and the overall GR yield and rate of CO in *n*CytcCO were similar to those in *c*CytcCO. The GR in both Cytc proteins was much more efficient than that in functional ligand-binding proteins such as Mb and Hb.[31,32] Highly inefficient GR of CO to Mb has been attributed to the structure of its PDS, which suppresses the GR of CO by holding the dissociated CO for longer than tens of nanoseconds, orientationally and spatially restricting the CO motion from rebinding.[5,9,10,40−42] Although the structure near the active site of the folded Cytc is well organized, it does not have a functional structure equivalent to the PDS found in Mb.[13,43] The GR of CO to folded Cytc was found to be even faster than that to a model heme, Mp, in viscous solvent.[10,44] The GR of CO to Mp became faster as the solvent grew more viscous.[44] This observation indicated that the GR of CO becomes more efficient as the diffusion of the dissociated CO is retarded, keeping it near the active site for a longer period. The organized protein matrix in folded Cytc can serve as an efficient trap for the dissociated CO that keeps the ligand near the Fe atom for a longer period. Clearly, the organized protein matrix in folded Cytc is a more efficient trap for the dissociated CO than a viscous but structureless solvent medium, resulting in faster and more efficient GR of CO in folded Cytc.[10] A narrower vibrational band in *n*CytcCO suggests that dislocated Met-80 in *n*Cytc has a narrower distribution in the distal conformation than chemically modified and dislocated Met-80 in *c*Cytc. Carboxymethylation of the sulfur atom of Met-80 in *c*Cytc would make the residue bulkier, and thus, more extensively perturb the distal pocket of the native structure. Slightly conformation-dependent GR of CO in *n*Cytc and *c*Cytc is consistent with the notion that the protein matrix in folded Cytc serves as a trap for the dissociated ligand. Since different conformations, particularly in the distal side of the heme, result in various traps, the GR of CO would, to a certain degree, depend on the conformation of the protein. In any event, the organized protein matrix certainly hinders the diffusion of the dissociated CO away from the Fe atom, and thus, the GR of CO to folded Cytc is very efficient, as observed. As can be seen in Figure 7, a small portion of the CO dissociated from *n*CytcCO escaped to the solvent on the picosecond time scale. The picosecond escape of the dissociated CO was suggested to occur through a small opening in the distal side of the folded Cytc, observed in a solution NMR structure study of ligand-bound Cytc.[43] It was suggested that, except for the CO that escaped into the bulk solution, most of the CO trapped inside the folded protein was geminately rebound in 1 ns.[10] The fraction of the deligated CO that escaped into bulk solution in *n*CytcCO, 0.14, is lower than that in *c*CytcCO, as shown in Figure 5, but similar to 0.11, the value reported for *c*CytcCO using transient optical spectroscopy.[11] The variation in the escaped fraction in *c*CytcCO was attributed to the degree of incubation with bromoacetic acid during chemical modification of the protein.[11] In case of Cytc−cardiolipin complex, found in the initial stages of apoptosis, only 20% of the deligated CO geminately rebinds on the picosecond time scale.[45] The drastic change in the GR yield was attributed to substantial change in protein flexibility and conformation upon the interaction of Cytc with cardiolipin.[45] Clearly, the GR yield of CO depends on the conformation of the protein.

Whereas a majority of the dissociated CO geminately rebound in folded Cytc, a small fraction of dissociated CO geminately rebound to *u*Cytc in 1 ns. As can be seen in Figures 4 and 7, the decay kinetics of the C_α band was virtually identical to that of the A_6 band and the fraction of the A_6 band in the A band was the same as that of the C_α band in the vibrational band of the photodeligated CO. This implies that the conformation of *u*CytcCO for the A_6 band results in the C_α band when the CO is deligated. The fraction of the A_6 band in *u*CytcCO decreased from 30 to 5% as the protein concentration decreased from 9 to 0.3 mM. Although not measured, the fraction of the C_α band in the time-resolved spectra of the deligated CO was expected to decrease with decreasing protein concentration. More than half of the CO dissociated from 9 mM *u*CytcCO escaped to the solvent within 1 ns, and the ligand escape proceeded on a picosecond time scale. Because there was no GR in 1 ns in the remaining two A bands in *u*CytcCO (A_5 and A_7 bands), they must be related to the C_S and C_β bands. If the conformation for the A_6 band, which increases with protein concentration, arises from soluble aggregates of *u*CytcCO, then the monomeric unfolded CytcCO has a structure that does not undergo GR of CO in 1 ns. The deligated CO from the monomeric unfolded CytcCO appears to be ill-trapped and thus diffuses away into the solvent without GR. Evidently, the distal part in monomeric *u*Cytc, far from organized and highly inhomogeneous, is very inefficient in trapping the dissociated CO, so that the CO cannot undergo GR in 1 ns.

As mentioned above, the efficiency of the GR of CO increases as the dissociated CO is more efficiently trapped near the Fe atom after photolysis. Virtually every deligated CO in the conformation for the A_6 band of *u*CytcCO rebinds geminately with a mean time constant of 160 ps, similar to the mean time constant of 140 ps in *n*CytcCO. The dissociated CO in *u*CytcCO that geminately rebinds appears to be as well trapped as that in the folded CytcCO. Clearly, the aggregated *u*CytcCO provides a trap for the deligated CO as efficient as the folded CytcCO. The absence of CO escape into the solvent from the conformation with the A_6 band of *u*CytcCO suggests that the *u*CytcCO aggregate is structured such that the deligated CO is trapped and cannot escape into the solvent, similarly to the CO trapped in the folded CytcCO. As can be seen in Figure 7, a few picoseconds are required for the C_S band to appear. Since CO bound to heme is known to be photodeligated within 0.1 ps,[30] the delayed appearance of the C_S band indicates that the solvation of the CO takes a few picoseconds. Although the monomeric *u*CytcCO seems to have unfolded random structures that cannot trap the deligated CO to a degree that the CO rebinds geminately, the bound CO is not exposed to the solvent. The rebinding kinetics of the dissociated CO to *u*Cytc suggests that monomeric *u*CytcCO has a loose structure that does not expose the bound CO to the solvent but cannot trap the deligated CO to rebind geminately. The soluble aggregate of *u*CytcCO that is formed as the protein concentration increases has a distal structure that makes the entire deligated CO geminately rebind as efficiently as the folded CytcCO.

As can be seen in Figures 6 and 7, solvated CO starts to appear a few picoseconds after photodeligation. If the CO bound in CytcCO is exposed to the solvent, the solvated CO will appear immediately after photodeligation. Clearly, the CO of CytcCO is not exposed to the solvent even under extreme denaturation conditions, for example, in the presence of 7 M GdnHCl, which implies that the CO ligand is buried inside hydrophobic residues of the unfolded protein.[46] A cofactor in metalloproteins is often

dx.doi.org/10.1021/jp401481q | J. Phys. Chem. B 2013, 117, 4934−4944

essential to stabilize their native structures.[47−49] For example, Mb folds into a marginally stable state without its cofactor, heme. In contrast, Cyt resembles a disordered apoprotein without heme,[50,51] and covalent attachment of the heme initiates its folding into the native structure.[52,53] The rebinding dynamics of CO to *u*Mb suggested that the CO in the unfolded MbCO is also buried inside the hydrophobic residues of the protein.[5] Clearly, the heme cofactor in heme proteins is sufficiently hydrophobic that it is buried within the hydrophobic residues of the protein even in highly concentrated denaturant. Therefore, typical descriptions that depict denatured CytcCO with the bound CO completely exposed to the solvent, like those found in Figures 2 of refs 15 and 54, are misleading.

We found that some portion of *n*CytcCO underwent irreversible photodeligation, that is, the population of *n*CytcCO gradually decreased as the photodeligation experiment proceeded. Evidently, some of the deligated CO did not rebind to the protein. This is consistent with the fact that *n*CytcCO is not in thermal equilibrium, and there is a slow CO thermal dissociation.[48] The half-life for the thermal dissociation of the CO ligand from CytcCO in 1.8 M GdnHCl (*n*CytcCO → *n*Cytc + CO) is 6.4 h at 283 K,[48] our experimental temperature; thus, more than 90% of the protein remains CO-ligated within one hour after sample preparation. To minimize the influence of thermal dissociation, all measurements were carried out within one hour of *n*CytcCO sample preparation. The sample was also flowed from a large quantity of stock to minimize the influence of irreversible photodeligation. Furthermore, the time-sequence data were collected in a round-trip manner over a short time, and the collection was repeated to obtain the necessary S/N ratio to minimize the influence of the gradual decrease in the quantity of the ligated sample on the rebinding kinetics. We found that the decrease in the ligated sample was less than 3% after one round trip in the time sequence. The gradual decrease in the quantity of *n*CytcCO overestimates the decay of the rebinding kinetics. However, the error introduced to the recovered kinetics under our experimental conditions was estimated to be about 1%. In contrast to *n*CytcCO, *c*CytcCO and *u*CytcCO are in thermal equilibrium, and thus it was not necessary to flow these samples. They were rotated, since flowing requires a large quantity of the sample. The rebinding of CO to *c*Cytc is similar to that to *n*Cytc, even though *c*CytcCO is in thermal equilibrium and *n*CytcCO is not. Therefore we may say that the GR of CO to folded Cytc critically relies on the structure in the distal cavity of the protein that traps the dissociated CO, and the structure does not crucially depend on the thermodynamic stability of the CO-bound protein. Interestingly, the thermodynamic stability differentiates not the GR but the bimolecular rebinding of CO to *n*Cytc from that to *c*Cytc.

The appearance of the C_S band in *c*Cytc on a time scale of tens of picoseconds was attributed to the ultrafast escape of the dissociated CO to the bulk solution through the small opening in the active site of the protein. In *n*Cytc, the C_S band also appears within a few tens of picoseconds, suggesting that the folded *n*Cytc has an opening in the distal part of its active site, too.[10] Because the details of the rebinding kinetics of *n*Cytc are similar to those of *c*Cytc, it is likely that the overall structure of *n*Cytc is similar to that of *c*Cytc. Of course, the chemically modified protein, *c*Cytc, may have a slightly more random structure in the distal area to accommodate the bulkier carboxymethyl group attached to the Met-80. However, the similarity in its spectra of dissociated CO as well as in its rebinding dynamics suggests that *n*Cytc has an overall structure that is likely the same as that of *c*Cytc. Therefore, we can conclude that native Cytc does not have a PDS-like structure that is found in native Mb and that the PDS is a characteristic of ligand-bound proteins such as Mb and Hb.[9,26]

After photodissociation from CytcCO, the dissociated CO geminately rebinds, translocates between internal cavities, or diffuses away to the solvent. Since neither the diffusion nor the translocation is synchronized, the actual motion cannot be observed. Initially, the dissociated CO can be distributed among multiple locations before it settles into internal cavities.[55] When the dissociated CO is distributed among multiple locations where the spectral characteristics of CO are not similar, the spectra for these CO molecules are inhomogeneously broadened, and thus, their spectral features are likely too small to be detectable. Apparent spectral bands are detected only when a measurable fraction of the ligand has accumulated in specific sites at some point in time.[41] When the dissociated CO is translocating or diffusing between sites or is located in multiple inhomogeneous locations, the spectral band may not have a detectable magnitude.[10] As observed in *c*CytcCO, the total integrated area of the vibrational spectrum of the dissociated CO is not scalable to that of the bleach spectrum of the corresponding protein (top panels of Figure 7). The discrepancy in the total integrated area was attributed to the existence of the undetectable states of the dissociated CO (denoted as the U state).[5,10]

The integrated absorbance for the dissociated CO depends on the extent of the librational motion of CO in the corresponding site[25,56,57] as well as the population of CO in the site. The librational motion of CO is governed by the spatial constraint imposed by the surrounding protein residues.[9] Because the protein residues rearrange after photodeligation, the integrated absorbance can grow without a corresponding population change as the spatial constraint establishes. For example, the integrated absorbance of the CO dissociated from MbCO grows within 1.1−1.6 ps due to protein rearrangement around the B state after CO translocation.[9,22] After the initial growth, the integrated absorbance of the B state in Mb remains the same during the conformational relaxation of the protein.[9,22] The rearrangement of protein residues is also expected in the folded protein *n*CytcCO. The spectral intensity of the CO dissociated from *n*CytcCO can grow, since it takes time to fully establish cavities for the CO. The protein rearrangement around the C site, if any, probably proceeds within 1−2 ps. Thus, the integrated absorbance of the C site in folded Cytc is proportional to the population of the corresponding site after 1−2 ps.

The extinction coefficients of the two B states in Mb were found to be the same,[24] but the extinction coefficient of the CO band in water was 0.6 times smaller than that in the B state.[38] Here, for the sake of simplicity, we assumed that the integrated absorbance of a state is proportional to the CO population of the corresponding state, the extinction coefficients of the two C bands in *u*CytcCO (C_α and C_β) are the same, and the extinction coefficient of the C_S band is either 0.6 times smaller than or equal to that of the other C band (C_1 band in *n*CytcCO and C_α or C_β band *u*CytcCO).

The kinetics of the C states of CytcCO can be used to obtain the GR rates from each state and the transition rates among them. As discussed above, since not all the dissociated CO appears in C states, the U state was introduced to account for the population of dissociated CO that cannot form a detectable spectral feature. Various kinetic schemes were tried to fit the kinetics of the C states under the constraint of satisfying the

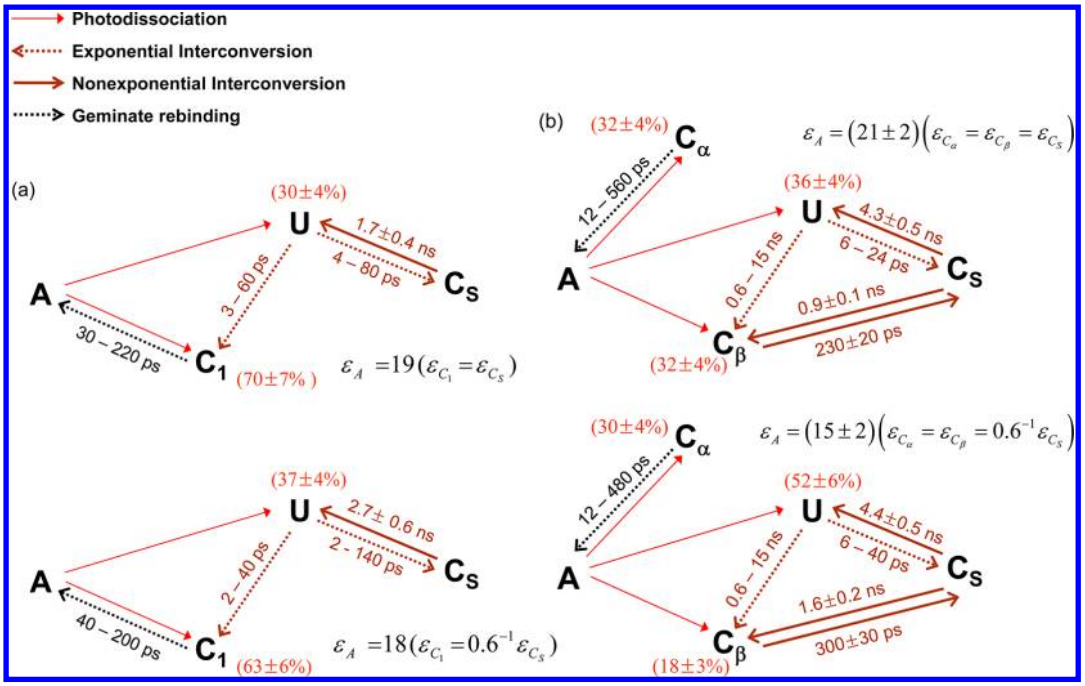

Figure 8. Best kinetic scheme with fitted parameters found by globally fitting the whole spectra of the CO dissociated from and bound to *n*CytcCO (a) and concentrated *u*CytcCO (b) at 283 K. The kinetic scheme allows transitions among and rebinding from all three states (C_1, C_S, and U) for *n*CytcCO or four states (C_α, C_β, C_S, and U) for *u*CytcCO with nonexponential rates. It was assumed that the extinction coefficient of the C_S band is equal to (upper scheme) or 0.6 times (lower scheme) that of the other C bands (C_1 band in *n*CytcCO, and C_α and C_β bands in *u*CytcCO). The extinction coefficient of the C_α band was assumed to be the same as that of the C_β band (see text). The extinction coefficient of the C_i band was denoted as ε_{Ci}. The fitted ratio of the extinction coefficient for the bound CO (ε_A) to that of the dissociated CO was found to be 15−21. Those time constants that were too long to be of any consequence were removed from the fit. Nonexponential kinetics was described by the stretched exponential function, and its parameters are shown by the time-dependent rates calculated at 0.3 ps and 1 ns. Time constants for the rates are shown along the arrow. Values in red shown in parentheses are the nascent partitioning of the photolyzed CO. The quoted uncertainties reflect fitting error and estimated experimental error.

overall change of the A state. The most general kinetic scheme allows transitions among all three states (C_1, C_S, and U) for *n*CytcCO or four states (C_α, C_β, C_S, and U) for the concentrated *u*CytcCO and rebinding from all the states of the corresponding protein. Even this most general kinetic model cannot reproduce the kinetics of each C state if all the kinetics are set to be exponential, suggesting that nonexponential kinetics are required to reproduce the kinetic behavior of the C states. Nonexponential kinetics can result from protein conformational relaxation after photodeligation,[58] distribution of rates due to the structural inhomogeneity of the protein,[59] or diffusive motion of the dissociated ligand. We used a stretched exponential function, $\exp(-(kt)^\beta)$ to describe the nonexponential kinetic behavior.[35,36,60,61] Here, the stretched exponential function represents a distribution of rates and/or a time-dependent rate. The mean time constants from the distribution can be calculated as $\langle\tau\rangle = \Gamma(\beta^{-1})/\beta k$, and the time-dependent rate coefficient, as $k(t) = k^\beta t^{\beta-1}$.[62]

Figure 8 shows the best kinetic schemes found by global fitting of the whole spectra of the dissociated CO and the overall change of bound CO in *n*CytcCO and the concentrated *u*CytcCO. These schemes may not be unique solutions for the kinetics of the CO dissociated from the corresponding proteins, but they can serve as a good working model. A similar kinetic scheme was used to describe the kinetic behavior of *c*CytcCO. Since the integrated area can grow with a 1−2 ps time constant because of the rearrangement of the surrounding residues, and our data range up to 1 ns, there might be larger errors in the fitted time constants for the ranges of a few ps or larger than 1 ns. Although the fitted parameters depend on how the extinction coefficient of the CO band in water was set relative to the other bands for the dissociated CO (0.6 times or equal), the dynamics of the dissociated CO remains the same. A value of 15−21 was found for the ratio of the extinction coefficient of the vibrational band for the bound CO to that for the dissociated CO. This value is about 2 times smaller than that for MbCO[25] but similar to that for *c*CytcCO.[10] For *n*CytcCO, the nascent partitioning of the dissociated CO was fitted to 63−70% in C_1 and 30−37% in U (figure 8a). According to this kinetic scheme, about 30−37% of the photodissociated CO is initially undetectable and gradually goes into either the C_1 site or solvent nonexponentially. The CO in the solvent goes into the undetectable state with a 2−3 ns time constant. The nonexponential loss of CO in the C_1 site is solely from rebinding, and CO rebinds primarily from the C_1 site. The C_1 site was envisioned as hydrophobic sites accumulating a measurable CO population near the heme Fe. The kinetic scheme for *n*CytcCO is virtually the same as that for *c*CytcCO, where a fraction of the dissociated CO goes into solvent ballistically through a small opening in the active site and the remainder is trapped near the Fe atom by the organized protein matrix and geminately rebinds. For concentrated *u*CytcCO, the nascent partitioning of the dissociated CO is fitted to about 30−32% in C_α, 18−32% in C_β, and 36−52% in U (Figure 8b). In this kinetic scheme, about 30% of the dissociated CO is trapped in the C_α site, where all of it nonexponentially rebinds. The GR to *u*Cytc solely comes from the dissociated CO in the C_α site. About 36−52% of the photodissociated CO is initially undetectable and goes into the C_β site or into solvent nonexponentially. The CO in the solvent goes to the undetectable state or the C_β site exponentially. The CO in the C_β site does not rebind and is in

dx.doi.org/10.1021/jp401481q | J. Phys. Chem. B 2013, 117, 4934−4944

equilibrium with that in the solvent. As discussed above, the C_α site likely represents hydrophobic cavities that are formed by aggregation of the unfolded CytcCO. The C_β site may represent those hydrophobic cavities that accumulate a measurable CO population but are so loosely arranged that the CO in the C_β site cannot rebind and only goes back and forth to the solvent. The CO in solvent goes either directly to the C_β site or to an undetectable site. In the above kinetic scheme, the motion of CO from the C_S state is not bimolecular but geminate because the CO is returning to its binding protein. As mentioned bimolecular rebinding is known to require a millisecond time scale, and thus the rebinding of CO observed in our experiment results only from the geminate type.

CONCLUSIONS

The GR dynamics of the CO photodeligated from *n*CytcCO (CytcCO in 1.8 M GdnHCl) is similar to that from *c*CytcCO, a CO-ligated Cytc with a carboxymethylated sulfur atom of Met-80. As was observed in *c*CytcCO, a small fraction of the CO dissociated from *n*CytcCO escapes into the bulk solvent on the picoseconds time scale, and most of the remaining CO undergoes efficient GR within 1 ns, suggesting that *n*CytcCO has a similar overall structure to that of *c*CytcCO. We can say that *n*CytcCO has a small opening in the distal side of the protein, the organized protein matrix acts as an efficient trap for the dissociated CO with no facile CO pathway into the protein matrix, and *n*CytcCO has no structure akin to the PDS found in Mb, which suppresses the GR of CO by holding the dissociated CO in a fashion unfavorable for binding.

The GR yield of CO to completely unfolded Cytc by 7 M GdnHCl increases from 5 to 30% as the protein concentration increases from 0.3 to 9 mM. The photodeligation of CO in 9 mM *u*CytcCO shows that about 30% of the dissociated CO undergoes GR as efficiently as that in the folded counterpart, and the majority of the remaining CO escapes to the solvent on a picosecond time scale. However, there is no immediate appearance of CO in the solvent. These observations suggest the following. (1) A fraction of the unfolded CytcCO forms a soluble aggregate that induces the deligated CO to geminately rebind as efficiently as the folded CytcCO. (2) The monomeric unfolded protein has a loose and/or random structure, and thus the dissociated CO escapes into solvent without GR. (3) CO bound to the monomeric unfolded protein is surrounded by the hydrophobic residues of the unfolded protein, as depicted in ref 46, even under complete unfolding conditions. Our data suggest that CytcCO in a high concentration of GdnHCl does not have the fully extended structure with exposed CO, as depicted in several literature reports[15,54] and it can form a soluble aggregate even at a protein concentration of a few tenths mM and under high denaturant concentrations.

AUTHOR INFORMATION

Corresponding Author

*E-mail: mhlim@pusan.ac.kr.

Notes

The authors declare no competing financial interest.

ACKNOWLEDGMENTS

This work was supported by the National Research Foundation of Korea (NRF) grant funded by the Korea government (MEST) (No. 2011-0016114). J.K. was supported by the 2012 Post-Doc Development Program of Pusan National University.

REFERENCES

(1) Dobson, C. M. The Structural Basis of Protein Folding and Its Links with Human Disease. *Philos. Trans. R. Soc. London, Ser. B* **2001**, *356*, 133−145.
(2) Klein-Seetharaman, J.; Oikawaz, M.; Grimshaw, S. B.; Wirmer, J.; Duchardt, E.; Ueda, T.; Imoto, T.; Smith, L. J.; Dobson, C. M.; Schwalbe, H. Long-Range Interactions within a Nonnative Protein. *Science* **2002**, *295*, 1719−1722.
(3) Shortle, D.; Ackerman, M. S. Persistence of Native-Like Topology in a Denatured Protein in 8 M Urea. *Science* **2001**, *293*, 487−489.
(4) Dobson, C. M.; Sali, A.; Karplus, M. Protein Folding: A Perspective from Theory and Experiment. *Angew. Chem., Int. Ed.* **1998**, *37*, 869−893.
(5) Park, J.; Kim, J.; Lee, T.; Lim, M. Dynamics of Ligand Rebinding to Unfolded MbCO by Guanidine HCl. *Biophys. J.* **2008**, *94*, L84−L86.
(6) Antonini, E.; Brunori, M. Hemoglobin and Myoglobin in Their Reactions with Ligands. *Front Biol* **1971**, *21*, 47.
(7) Austin, R. H.; Beeson, K. W.; Eisenstein, L.; Frauenfelder, H.; Gunsalus, I. C. Dynamics of Ligand Binding to Myoglobin. *Biochemistry* **1975**, *14*, 5355−5373.
(8) Springer, B. A.; Sligar, S. G.; Olson, J. S.; Phillips, G. N., Jr. Mechanisms of Ligand Recognition in Myoglobin. *Chem. Rev.* **1994**, *94*, 699−714.
(9) Lim, M.; Jackson, T. A.; Anfinrud, P. A. Ultrafast Rotation and Trapping of Carbon Monoxide Dissociated from Myoglobin. *Nat. Struct. Biol.* **1997**, *4*, 209−214.
(10) Kim, J.; Park, J.; Lee, T.; Lim, M. Dynamics of Ultrafast Rebinding of CO to Carboxymethyl Cytochrome c. *J. Phys. Chem. B* **2009**, *113*, 260−266.
(11) Silkstone, G.; Jasaitis, A.; Vos, M. H.; Wilson, M. T. Geminate Carbon Monoxide Rebinding to a c-Type Haem. *Dalton Trans.* **2005**, 3489−3494.
(12) Schejter, A.; George, P. Production of A "Cytochrome c" With Myoglobin-Like Properties by Alkylating the Cyanide Complex with Bromoacetate. *Nature* **1965**, *206*, 1150−1151.
(13) Silkstone, G.; Jasaitis, A.; Wilson, M. T.; Vos, M. H. Ligand Dynamics in an Electron Transfer Protein. Picosecond Geminate Recombination of Carbon Monoxide to Heme in Mutant Forms of Cytochrome c. *J. Biol. Chem.* **2007**, *282*, 1638−1649.
(14) Wang, W.; Ye, X.; Demidov, A. A.; Rosca, F.; Sjodin, T.; Cao, W.; Sheeran, M.; Champion, P. M. Femtosecond Multicolor Pump-Probe Spectroscopy of Ferrous Cytochrome c. *J. Phys. Chem. B* **2000**, *104*, 10789−10801.
(15) Jones, C. M.; Henry, E. R.; Hu, Y.; Chan, C. K.; Luck, S. D.; Bhuyan, A.; Roder, H.; Hofrichter, J.; Eaton, W. A. Fast Events in Protein Folding Initiated by Nanosecond Laser Photolysis. *Proc. Natl. Acad. Sci. U.S.A.* **1993**, *90*, 11860−11864.
(16) Eaton, W. A.; Thompson, P. A.; Chan, C.-K.; Hagen, S. J.; Hofrichter, J. Fast Events in Protein Folding. *Structure* **1996**, *4*, 1133−1139.
(17) Fleming, P. J.; Rose, G. D. Conformational Properties of Unfolded Proteins. *Protein Folding Handb.* **2005**, *2*, 706−736.
(18) Tanford, C. Protein Denaturation. *Adv. Protein Chem.* **1968**, *23*, 121−282.
(19) Tanford, C. Protein Denaturation. C. Theoretical Models for the Mechanism of Denaturation. *Adv. Protein Chem.* **1970**, *24*, 1−95.
(20) Tanford, C.; Pain, R. H.; Otchin, N. S. Equilibrium and Kinetics of the Unfolding of Lysozyme (Muramidase) by Guanidine Hydrochloride. *J. Mol. Biol.* **1966**, *15*, 489−504.
(21) Kim, S.; Chung, J. K.; Kwak, K.; Bowman, S. E. J.; Bren, K. L.; Bagchi, B.; Fayer, M. D. Native and Unfolded Cytochrome c - Comparison of Dynamics Using 2D-IR Vibrational Echo Spectroscopy. *J. Phys. Chem. B* **2008**, *112*, 10054−10063.
(22) Kim, S.; Heo, J.; Lim, M. Conformational Dynamics of Heme Pocket in Myoglobin and Hemoglobin. *Bull. Korean Chem. Soc.* **2005**, *26*, 151−156.
(23) Kim, S.; Lim, M. Protein Conformation-Induced Modulation of Ligand Binding Kinetics: A Femtosecond Mid-Ir Study of Nitric Oxide Binding Trajectories in Myoglobin. *J. Am. Chem. Soc.* **2005**, *127*, 8908−8909.

(24) Kim, S.; Lim, M. Picosecond Dynamics of Ligand Interconversion in the Primary Docking Site of Heme Proteins. *J. Am. Chem. Soc.* **2005**, *127*, 5786−5787.
(25) Lim, M.; Jackson, T. A.; Anfinrud, P. A. Mid-Infrared Vibrational Spectrum of CO after Photodissociation from Heme: Evidence for a Ligand Docking Site in the Heme Pocket of Hemoglobin and Myoglobin. *J. Chem. Phys.* **1995**, *102*, 4355−4366.
(26) Lim, M.; Jackson, T. A.; Anfinrud, P. A. Orientational Distribution of CO before and after Photolysis of MbCO and HbCO: A Determination Using Time-Resolved Polarized Mid-IR Spectroscopy. *J. Am. Chem. Soc.* **2004**, *126*, 7946−7957.
(27) Kim, S.; Jin, G.; Lim, M. Dynamics of Geminate Recombination of NO with Myoglobin in Aqueous Solution Probed by Femtosecond Mid-Ir Spectroscopy. *J. Phys. Chem. B* **2004**, *108*, 20366−20375.
(28) Chung, J. K.; Thielges, M. C.; Bowman, S. E. J.; Bren, K. L.; Fayer, M. D. Temperature Dependent Equilibrium Native to Unfolded Protein Dynamics and Properties Observed with IR Absorption and 2D IR Vibrational Echo Experiments. *J. Am. Chem. Soc.* **2011**, *133*, 6681−6691.
(29) Kim, J.; Park, J.; Chowdhury, S. A.; Lim, M. Picosecond Dynamics of CN^--Ligated Ferric Cytochrome c after Photoexcitation Using Time-Resolved Vibrational Spectroscopy. *Bull. Korean Chem. Soc.* **2010**, *31*, 3771−3776.
(30) Petrich, J. W.; Poyart, C.; Martin, J. L. Photophysics and Reactivity of Heme Proteins: A Femtosecond Absorption Study of Hemoglobin, Myoglobin, and Protoheme. *Biochemistry* **1988**, *27*, 4049−4060.
(31) Henry, E. R.; Sommer, J. H.; Hofrichter, J.; Eaton, W. A. Geminate Recombination of Carbon Monoxide to Myoglobin. *J. Mol. Biol.* **1983**, *166*, 443−451.
(32) Murray, L. P.; Hofrichter, J.; Henry, E. R.; Ikeda-Saito, M.; Kitagishi, K.; Yonetani, T.; Eaton, W. A. The Effect of Quaternary Structure on the Kinetics of Conformational Changes and Nanosecond Geminate Rebinding of Carbon Monoxide to Hemoglobin. *Proc. Natl. Acad. Sci. U.S.A.* **1988**, *85*, 2151−2155.
(33) Ansari, A.; Berendzen, J.; Braunstein, D. K.; Cowen, B. R.; Frauenfelder, H.; Hong, M. K.; Iben, I. E. T.; Johnson, J. B.; Ormos, P.; Sauke, T. B.; Scholl, R.; Schulte, A.; Steinbach, P. J.; Vittitow, J.; Young, R. D. Rebinding and Relaxation in the Myoglobin Pocket. *Biophys. Chem.* **1987**, *26*, 337−355.
(34) Muller, J. D.; McMahon, B. H.; Chien, E. Y.; Sligar, S. G.; Nienhaus, G. U. Connection between the Taxonomic Substates and Protonation of Histidines 64 and 97 in Carbonmonoxy Myoglobin. *Biophy. J.* **1999**, *77*, 1036−1051.
(35) Cao, W.; Ye, X.; Georgiev, G. Y.; Berezhna, S.; Sjodin, T.; Demidov, A. A.; Wang, W.; Sage, J. T.; Champion, P. M. Proximal and Distal Influences on Ligand Binding Kinetics in Microperoxidase and Heme Model Compounds. *Biochemistry* **2004**, *43*, 7017−7027.
(36) Lee, K. C. B.; Siegel, J.; Webb, S. E. D.; Leveque-Fort, S.; Cole, M. J.; Jones, R.; Dowling, K.; Lever, M. J.; French, P. M. W. Application of the Stretched Exponential Function to Fluorescence Lifetime Imaging. *Biophys. J.* **2001**, *81*, 1265−1274.
(37) Sagnella, D. E.; Straub, J. E.; Jackson, T. A.; Lim, M.; Anfinrud, P. A. Vibrational Population Relaxation of Carbon Monoxide in the Heme Pocket of Photolyzed Carbonmonoxy Myoglobin: Comparison of Time-Resolved Mid-IR Absorbance Experiments and Molecular Dynamics Simulations. *Proc. Natl. Acad. Sci. U.S.A.* **1999**, *96*, 14324−14329.
(38) Jackson, T. A.; Lim, M.; Anfinrud, P. A. Probing the Dynamics of Ligand Motion in Myoglobin with Femtosecond IR Spectroscopy; Department Chemistry, Harvard University: Cambridge, MA, 1997.
(39) Kim, S.; Lee, T.; Lim, M. Conformational Dynamics of Heme-Pocket in Myoglobin Encapsulated in Silica Sol-Gel Glasses. *Bull. Korean Chem. Soc.* **2007**, *28*, 339−342.
(40) Nienhaus, K.; Deng, P.; Kriegl, J. M.; Nienhaus, G. U. Structural Dynamics of Myoglobin: Effect of Internal Cavities on Ligand Migration and Binding. *Biochemistry* **2003**, *42*, 9647−9658.
(41) Schotte, F.; Soman, J.; Olson, J. S.; Wulff, M.; Anfinrud, P. A. Picosecond Time-Resolved X-Ray Crystallography: Probing Protein Function in Real Time. *J. Struct. Biol.* **2004**, *147*, 235−246.
(42) Srajer, V.; Ren, Z.; Teng, T.-Y.; Schmidt, M.; Ursby, T.; Bourgeois, D.; Pradervand, C.; Schildkamp, W.; Wulff, M.; Moffat, K. Protein Conformational Relaxation and Ligand Migration in Myoglobin: A Nanosecond to Millisecond Molecular Movie from Time-Resolved Laue X-Ray Diffraction. *Biochemistry* **2001**, *40*, 13802−13815.
(43) Yao, Y.; Qian, C.; Ye, K.; Wang, J.; Bai, Z.; Tang, W. Solution Structure of Cyanoferricytochrome c: Ligand-Controlled Conformational Flexibility and Electronic Structure of the Heme Moiety. *J. Biol. Inorg. Chem.* **2002**, *7*, 539−547.
(44) Park, J.; Lee, T.; Lim, M. Viscosity-Dependent Dynamics of CO Rebinding to Microperoxidase-8 in Glycerol/Water Solution. *J. Phys. Chem. B* **2010**, *114*, 10897−10904.
(45) Kapetanaki, S. M.; Silkstone, G.; Husu, I.; Liebl, U.; Wilson, M. T.; Vos, M. H. Interaction of Carbon Monoxide with the Apoptosis-Inducing Cytochrome c-Cardiolipin Complex. *Biochemistry* **2009**, *48*, 1613−1619.
(46) Choi, J.; Jung, Y. O.; Lee, J. H.; Yang, C.; Kim, B.; Ihee, H. Folding Dynamics of Ferrocytochrome c in a Denaturant-Free Environment Probed by Transient Grating Spectroscopy. *ChemPhysChem* **2008**, *9*, 2708−2714.
(47) Feng, Y. Q.; Wand, A. J.; Sligar, S. G. 1h and 15n NMR Resonance Assignments and Preliminary Structural Characterization of Escherichia Coli Apocytochrome B562. *Biochemistry* **1991**, *30*, 7711−7717.
(48) Latypov, R. F.; Maki, K.; Cheng, H.; Luck, S. D.; Roder, H. Folding Mechanism of Reduced Cytochrome c: Equilibrium and Kinetic Properties in the Presence of Carbon Monoxide. *J. Mol. Biol.* **2008**, *383*, 437−453.
(49) Lecomte, J. T. J.; Sukits, S. F.; Bhattacharya, S.; Falzone, C. J. Conformational Properties of Native Sperm Whale Apomyoglobin in Solution. *Protein Sci.* **1999**, *8*, 1484−1491.
(50) Fisher, W. R.; Taniuchi, H.; Anfinsen, C. B. Role of Heme in the Formation of the Structure of Cytochrome c. *J. Biol. Chem.* **1973**, *248*, 3188−3195.
(51) Stellwagen, E.; Rysavy, R.; Babul, G. Conformation of Horse Heart Apocytochrome c. *J. Biol. Chem.* **1972**, *247*, 8074−8077.
(52) Dumont, M. E.; Cardillo, T. S.; Hayes, M. K.; Sherman, F. Role of Cytochrome c Heme Lyase in Mitochondrial Import and Accumulation of Cytochrome c in Saccharomyces Cerevisiae. *Mol. Cell. Biol.* **1991**, *11*, 5487−5496.
(53) Gonzales, D. H.; Neupert, W. Biogenesis of Mitochondrial c-Type Cytochromes. *J. Bioenerg. Biomembr.* **1990**, *22*, 753−768.
(54) Kumar, R.; Prabhu, N. P.; Bhuyan, A. K. Ultrafast Events in the Folding of Ferrocytochrome C. *Biochemistry* **2005**, *44*, 9359−9367.
(55) Schmidt, M.; Nienhaus, K.; Pahl, R.; Krasselt, A.; Anderson, S.; Parak, F.; Nienhaus, G. U.; Srajer, V. Ligand Migration Pathway and Protein Dynamics in Myoglobin: A Time-Resolved Crystallographic Study on L29w MbCO. *Proc. Natl. Acad. Sci. U.S.A.* **2005**, *102*, 11704−11709.
(56) Helbing, J.; Nienhaus, K.; Nienhaus, G. U.; Hamm, P. Restricted Rotational Motion of CO in a Protein Internal Cavity: Evidence for Nonseparating Correlation Functions from IR Pump-Probe Spectroscopy. *J. Chem. Phys.* **2005**, *122*, 124505.
(57) Kriegl Jan, M.; Nienhaus, K.; Deng, P.; Fuchs, J.; Nienhaus, G. U. Ligand Dynamics in a Protein Internal Cavity. *Proc. Natl. Acad. Sci. U.S.A.* **2003**, *100*, 7069−7074.
(58) Steinbach, P. J.; Ansari, A.; Berendzen, J.; Braunstein, D.; Chu, K.; Cowen, B. R.; Ehrenstein, D.; Frauenfelder, H.; Johnson, J. B.; Lamb, D. C. Ligand Binding to Heme Proteins: Connection between Dynamics and Function. *Biochemistry* **1991**, *30*, 3988−4001.
(59) Petrich, J. W.; Lambry, J. C.; Kuczera, K.; Karplus, M.; Poyart, C.; Martin, J. L. Ligand Binding and Protein Relaxation in Heme Proteins: A Room Temperature Analysis of Nitric Oxide Geminate Recombination. *Biochemistry* **1991**, *30*, 3975−3987.
(60) Berberan-Santos, M. N.; Bodunov, E. N.; Valeur, B. Mathematical Functions for the Analysis of Luminescence Decays with Underlying Distributions 1. Kohlrausch Decay Function (Stretched Exponential). *Chem. Phys.* **2005**, *315*, 171−182.
(61) Frauenfelder, H.; Sligar, S. G.; Wolynes, P. G. The Energy Landscapes and Motions of Proteins. *Science* **1991**, *254*, 1598−1603.

(62) Jackson, T. A.; Lim, M.; Anfinrud, P. A. Complex Nonexponential Relaxation in Myoglobin after Photodissociation of MbCO: Measurement and Analysis from 2 ps to 56 micro s. *Chem. Phys.* **1994**, *180*, 131−140.